Separation Science and Technology
Publication details, including instructions for authors and subscription information:
http://www.informaworld.com/smpp/title~content=t713708471

Optimization of the Design and Operation of Seawater RO Desalination Plants

S. A. Avlonitis[a]
[a] Laboratory of Quality Control and Operations Management, Department of Mechanical Engineering, Technological Educational Institution (T.E.I.) of Halkidas, Greece

To cite this Article Avlonitis, S. A.(2005) 'Optimization of the Design and Operation of Seawater RO Desalination Plants', Separation Science and Technology, 40: 13, 2663 — 2678
To link to this Article: DOI: 10.1080/01496390500283415
URL: http://dx.doi.org/10.1080/01496390500283415

Separation Science and Technology, 40: 2663–2678, 2005

ISSN 0149-6395 print/1520-5754 online
DOI: 10.1080/01496390500283415

Optimization of the Design and Operation of Seawater RO Desalination Plants

S. A. Avlonitis
Laboratory of Quality Control and Operations Management,
Department of Mechanical Engineering, Technological Educational
Institution (T.E.I.) of Halkidas, Greece

Abstract: In this work a straightforward procedure for the optimum design and operation of the seawater reverse osmosis (SWRO) plants is being proposed. The analysis is based on analytical equations for the permeate flow rate and quality and the salt flow rate. The mathematical model and the developed software can predict the brine and permeate characteristics for any SWRO plant regardless of the number of the membrane modules in the pressure vessels. The results of the developed software were verified by experimental data from a $280\,m^3/d$ RO plant, with 8″ membrane module made by FilmTec, and they were compared with the predictions made by ROSA 6.0 software. An excellent agreement was observed between the prediction of the suggested model and the experimental data. The model can be applied in any type of membrane modules as long as the geometry and the membrane characteristics are known.

Different operating conditions were tested and an effort was made for the optimum design and operation of the plant so that the minimum specific energy consumption can be achieved. It is believed that the analytical model presented in this work is a very useful tool not only because of its accuracy for the SWRO plant design and operation but also because of its simplicity.

Keywords: Reverse osmosis plants, design, energy consumption, optimization

Received 30 March 2005, Accepted 25 July 2005
Address correspondence to S. A. Avlonitis, Laboratory of Quality Control and Operations Management, Department of Mechanical Engineering, Technological Educational Institution (T.E.I.) of Halkidas, 34400 Psaxna EVIA, Greece. Tel.: (22280) 99650; Fax: (22280) 99649; E-mail: savlon@teihal.gr

INTRODUCTION

Nowadays desalination by reverse osmosis is becoming the dominant method in the desalination area. New membranes, with high flux and low specific energy production (1, 2) and very efficient energy recovery systems, have been introduced in the market (3, 4). FilmTec SW30XLE-400 modules have shown an excellent performance and very high productivity at different locations and operating conditions (2). The optimal design of the membrane modules has been examined thoroughly by different researchers (5–10), using analytical or numerical methods. The next obvious step is the optimization of the design and the operation of the RO plants, especially for seawater treatment. This optimization process is always targeting to minimize the specific energy consumption of the desalinated seawater.

Several data for the specific energy consumption for seawater RO desalination plants have been already given by S. Avlonitis et al. (11). M. Wilf and K. Klinko (12) have suggested that the system recovery ratio has to be optimized with respect to membrane performance and process economics for the minimum desalinated water cost. A. A. Mesa et al. (13) have postulated that the autonomous electricity production for RO plants combined with MED plant results in 26% energy savings. The membrane type is a key factor for the optimization of the operation cost of an RO plant, reducing the energy consumption by 46% (14). The pretreatment procedure can be proved to be a key factor for the optimum RO plant performance (15). A new concept for the energy recovery system (PROP) has been introduced by T. Manth et al. (16). In this sophisticated and comprehensive approach the effects of variable parameters of operation in the specific energy consumption were considered. These parameters include flow rates at different recoveries, feed temperature and salinity with their resulting energy requirements, pressure losses caused by membrane fouling, and pressure losses caused by system controls such as feed throttle valves. Many computer programs have been developed to analyze the effect of the operating and design parameters on the recovery ratio and the efficiency of the system in the case of tubular RO membranes (17, 18). Similar computational procedures and theoretical models, for the analysis and optimization of the desalinated water production, have been proposed for dual purpose plants (19) or wastewater treatment by membrane procedures (20).

In this work a mathematical analytical model is being presented for the SWRO plants and a computer program has been written based on the developed equation for the formulation of the RO plant performance. The effects of various factors, such as recovery ratio, applied pressure, temperature, etc., have been examined on the RO plant performance and optimum operating conditions for the minimum specific energy consumption have been proposed, for plants with no energy recovery system and for membranes able to sustain the high pressure. The mathematical model has been compared with other models and verified by experimental data taken for a 280 m^3/d seawater RO plant.

MATHEMATICAL MODEL

The mathematical model is based on the equations of the average volumetric water flux, J, Eq. (1) and the average salt flux, J_2, Eq. (2), presented in previous work (6, 8, 9). In these equations the pressure drop in the permeate and brine channel, the concentration polarization and the concentration gradient along each membrane module and the pressure vessel have been taken into account with the approximations which are given in Table 1.

$$J = \frac{q \tan\mathrm{h}(w/q)}{\omega f w L}\left\{(k + k_1\omega c_f)\ln\frac{k + k_1\omega c_b(L)}{k + k_1\omega c_f}\left[\Delta P_{ef}(0, w) + \frac{k}{k_1}\right]\right.$$
$$- k\omega[c_B(L) - c_f] + \frac{c_f u_f k_{fb}\mu}{f}\left[k_1\omega(c_B(L) - c_f)\right.$$
$$\left.\left. -k\ln\frac{c_b(L)}{c_f}\ln\frac{k\omega(c_B(L) - c_f)}{k} - \frac{k_1^2\omega^2}{4k}(c_b^2(L) - c_f^2)\right]\right\} \tag{1}$$

$$J_2 = \frac{k_2}{wL}\left\{c_f wL + \frac{fL^2 w}{2} + \frac{q\tan\mathrm{h}(w/q)}{k_1 f\omega^2 k} \times \left\{k_1\omega(c_B(L) - c_f)\right.\right.$$
$$\times\left[\Delta P_{ef}(0, w)(k_1\omega c_f) + \frac{k^2}{k_1} - \frac{k\omega(c_B(L) - c_f)}{2}\right]$$
$$\times \ln\frac{k + k_1\omega c_B(L)}{k + k_1\omega c_f}\left[\Delta P_{ef}(0, w) + \frac{k}{k_1}\right] + \frac{k c_f u_1 k_{fb}\mu(c_B(L)/c_f)}{f}$$
$$\left.\left.\times\left[k\ln\frac{k + k_1\omega c_B(L)}{k} - k_1\omega c_B(L) + \frac{k_1^2\omega^2}{4k}(c_b^2(L) - c_f^2)\right]\right\}\right\} \tag{2}$$

where,

$$\Delta P_{ef}(0, w) = \frac{(\Delta P - \omega c_f)k}{k + k_1\omega c_f} \tag{3}$$

and

$$q = \sqrt{\frac{h_p}{2k_1 k_{fp}\mu}} \tag{4}$$

The average salt flux, J_2, is related to the average volumetric water flux, J, by Eq. (5). The permeate flow rate can be considered as the product of the total active membrane area (excluding the glued area of the membrane) and the

Table 1. Assumptions for the 2-dimension calculations

1. Validity of Darcy's law for permeate and brine channel.
2. Validity of solution-diffusion model, for the transport of water through the membrane. No flow restrictions for the locally produced permeate in the porous substructure of the composite membrane.
3. Immediate and complete mixing of the locally produced permeate water with the bulk flow in the permeate channel.
4. The permeate concentration has been neglected in comparison to the feed concentration.
5. Membrane modules are made up of flat channels, with constant geometrical shape, see appendix.
6. Constant fluid properties.
7. Negligible components of brine and permeate velocities along the y (tangential) and x (axial) axis, respectively.
8. Negligible diffusive mass transport along the x and y direction in both channels. This means that the flux through the membrane due to diffusion is much smaller to the flux due to convection. The driving force for the water transport is the effective pressure across the membrane.
9. The brine concentration varies linearly with the distance L, in the axial direction.

$$c_b = c_f + fx \tag{A.1}$$

where,

$$f = \frac{c_b(L) - c_f}{L} \tag{A.2}$$

The value of f is an indication of the recovery ratio R.

10. Validity of the thin film theory, with the approximation which is given by equation (A.3).

$$c_{bw} = c_b(1 + \frac{J}{k}) \tag{A.3}$$

11. A constant mass-transfer coefficient, given by equation A.4

$$Sh = 0.63 \times Sc^{0.17} \times \mathrm{Re}_f^{0.40} \times \left[\frac{c_f}{\rho}\right]^{-0.77} \times \left[\frac{P_f}{P_o}\right]^{-0.55} \tag{A.4}$$

12. Osmotic pressure proportional to the concentration, see equation (A.5).

$$\pi = \omega \times c \tag{A.5}$$

volumetric average water flux:

$$J_2 = Jc_p \tag{5}$$

For the calculations presented in this work the brine friction parameter, k_{fb}, was given by Eq. (6), the membrane permeability coefficient, k_1, by Eq. (7), the salt permeability coefficient by Eq. (8), and the permeate friction parameter was assumed constant at $k_{fp} = 1.1 \times 10^9 m^{-2}$.

$$k_{fb} = 309 \times \mathrm{Re}_f^{0.83} \tag{6}$$

$$k_1 = 4.3 \times 10^{-5} e^{8.6464\left(\frac{T-T_{20}}{T_{20}}\right)-0.0028P_f} \tag{7}$$

$$k_2 = 6.80 \times 10^{-7} \mathrm{e}^{14.648\frac{\mathrm{T}-\mathrm{T_o}}{\mathrm{T_o}}}. \tag{8}$$

These equations can be used as a straight and simple procedure to determine the permeate flow rate and the permeate quality of each individual membrane module. However, the same simple procedure can be applied even for a number of successive membrane modules, as they are in the real industrial membrane vessels. The mathematical model has the ability to make predictions about the permeate quantity and quality of each increment of any membrane module in the pressure vessels and the membrane module as a whole. Simple mass balances can give the permeate flow rate and permeate quality for more than one membrane modules; see Eq. (9).

$$Q_p = Q_{p1} + Q_{p2} + \ldots + Q_{pt}, \quad c_p = \frac{\sum_{i=1}^{t} c_{pi} Q_{pi}}{Q_p},$$
$$Q_{fi} = Q_{f(i-1)} - Q_{p(i-1)} \tag{9}$$

The same model can be used to determine optimum operating conditions for the minimum specific energy production. The specific energy consumption, ξ, can be identified as the ratio of the energy consumed divided by the volume of the produced water; see Eq. (10).

$$\xi = \frac{((P_1/n_1) + P_2) \times t}{Q_p \times t} = \frac{((P_1/n_1) + P_2)}{Q_p} = \frac{((P_1/n_1) + (\rho g Q_f \Delta h_{pump}/n_2))}{Q_p}$$
$$= \frac{P_1}{n_1 Q_p} + \frac{Q_f \Delta P_{pump}}{n_2 Q_p} = \frac{P_1}{n_1 Q_p} + \frac{\Delta P_{pump}}{n_2 R} \tag{10}$$

where P_1 is the power of the auxiliary devices of the SWRO plant and P_2 is the energy consumption of the high-pressure pump only; see Fig. 2.

CALCULATION PROCEDURE

The presented equations are applied for each individual membrane module. The water and solute flow rates as well as the permeate and brine concentrations and applied pressure are determined at the end of the first membrane modules. These output values are the input values for the second membrane module and so on. A simple mass balance will give the characteristics of the permeate water from the first, second, third, etc., membrane module. The following flow chart in Fig. 1 gives the algorithm of the calculations for the prediction of the plant performance.

RESULTS AND DISCUSSION

The experimental data were collected from a commercial plant with a capacity of 280 m^3/day, based in Santorini island in Greece and commissioned by

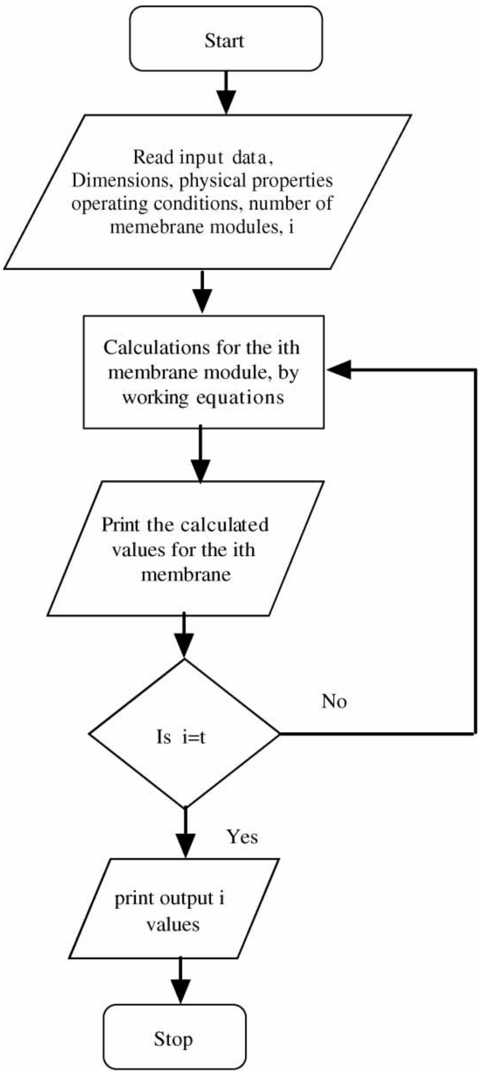

Figure 1. Logical diagram for the calculations.

Culligan in 2002. A simple flow chart of the core of the plant can be seen in Fig. 2. The plant has four pressure vessels with six membrane modules in each pressure vessel. The membrane modules are SW30HR-380 made by FilmTec. By the use of the feed and brine valves the recovery ratio and applied pressure could be controlled and experimental data were collected for different recovery ratios and different applied pressure. The effect of the feed temperature on permeate flux and quality was also examined, since data were collected for two different temperatures, 23°C and 19°C.

Three different data and prediction results concerning the plant performance are presented and compared in this work. These are:

- The experimental results, collected for the 280 m^3/day plant. Some of the data are given in Table 2.
- Predictions by the software ROSA 6.0 supplied by FilmTec.
- Predictions by the mathematical model presented in this work (software *Desal).*

The experimental data at 19°C and the predictions by *ROSA* 6.0 and *Desal* about the permeate flow rate and permeate concentration as well as the operating conditions are given in Table 2. The presented data are given in units more familiar to those working in commercial SWRO plants. The recoveries, for the three different data and predictions, are not exactly the same. The feed flow rate and pressure are kept the same but permeate flow rates are different, resulting in different recovery ratios. Both *Desal* and *ROSA* make

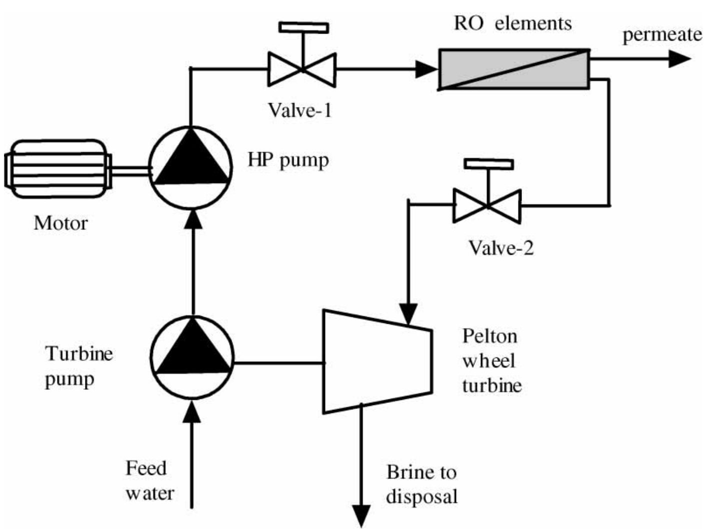

Figure 2. 280 m^3/day SWRO plant.

Table 2. Experimental data and predictions for the 280 m^3/day RO plant performance at 19°C

P_{feed} (bar)	Q_{feed} (m^3/h)	Q_p (m^3/h)			c_p (mg/lt)		
		Experimental	*ROSA*	*Desal*	Experimental	*ROSA*	*Desal*
63	43.50	12.50	11.61	12.02	191	174	214
61	40.70	11.70	10.71	11.12	210	188	228
58	33.80	9.80	9.09	9.65	250	221	265
57	39.50	10.00	9.28	9.78	215	210	247
52	35.90	7.90	7.30	7.86	270	258	292

reasonable predictions for the plant performance, although the plant is in operation for 2 years. The variation of the predicted results and the experimental data for permeate flow rate is 7.12%–8.46% for *ROSA* and 0.5%–4.95% for *Desal*. For the permeate concentration *ROSA*'s predictions (variation 2.3%–10.5%) are more accurate than *Desal*'s (variation 6%–14.8%) although the difference is not great. It must be noted that the plant is in operation for more than 2 years and possible fouling and scaling effects have been ignored in both performance predictions. If the scaling and fouling effects were taken into account it would be expected that the predicted values for the permeate flow rate would be even smaller and the permeate concentration even higher. The data for 23°C are illustrated in Figs 3 and 4. It is apparent that there is an excellent agreement between

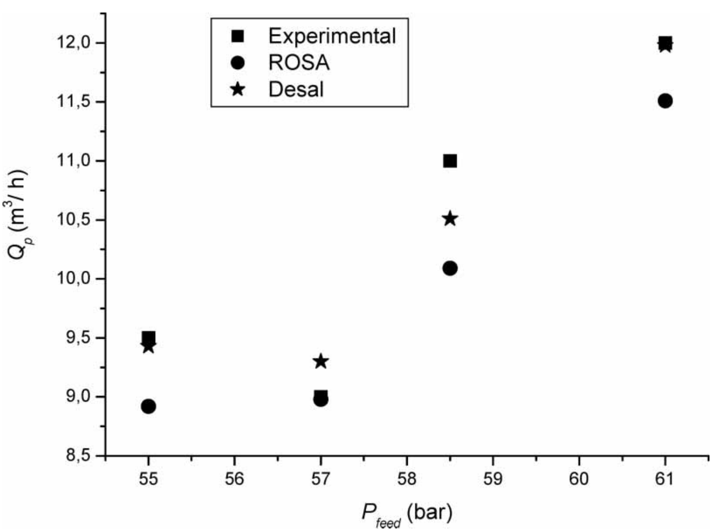

Figure 3. Permeate flow rates for different applied pressures at 23°C.

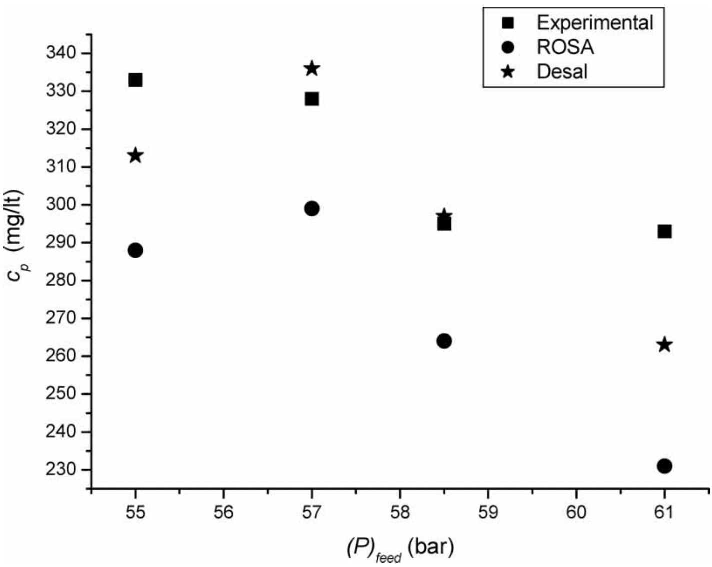

Figure 4. Permeate concentration for different applied pressures at 23°C.

Desal predictions and experimental data. The results are presented in units which are more common for commercial RO plants.

The energy consumption of the SWRO plant includes among the HP pump, the LP pump, the dosing pumps and the stirring devices. The characteristics of each energy consuming device of the plant are presented in Table 3.

The actual electric energy consumption was also recorded, and the experimental values of the specific energy consumption are presented in Table 4. In the same table the theoretical values by the use of Eq. (10) are also presented. It seems that Eq. (10) gives higher values of the specific energy consumption than the real ones. However, in a long-term experiment (32 days) the specific energy consumption for this plant was found to be 5.28 kWh/m^3 (9), including the pelton wheel turbine. In the previous specific energy consumption the startup and cleaning energy consumption were included. An explanation of the discrepancies between experimental results and predictions could be the

Table 3. Auxiliary devices and HP pump characteristics of the 280 m^3/day SWRO plant

Device	Head (m)	Capacity (m^3/h)	Power (kW)	Efficiency coefficient, n_1
LP pump	44	30	5.5	0,6
Stirrer	—	—	0.09	—
Five dosing pumps	—	—	2.2	0,8

Table 4. Specific energy consumption of the 280 m^3/day SWRO plant at 19°C

Q_f (m^3/h)	R	ΔP_{ef} (bar)	U_{rms} (V)	I_{rms} (A)	$\cos\varphi$	P (kW)	ξ (kWh/m^3) Experimental	ξ (kWh/m^3) Theoretical
40.70	0.287	61.00	415.00	108.00	0.95	42.58	3.64	4.91
43.50	0.287	63.00	415.00	111.00	0.95	43.76	3.50	4.57
33.80	0.290	58.00	415.00	102.00	0.95	40.21	4.10	5.02
39.50	0.253	57.00	415.00	106.00	0.95	41.79	4.18	4.96
35.90	0.220	52.00	415.00	103.50	0.95	40.80	5.17	5.32

existence of the energy recovery system. Its contribution to the reduction of the energy consumption is not clearly isolated from the actual energy consumption of the HP pump, when predictions were made by Eq. (10).

A more realistic evaluation of the credibility of the mathematical model presented in this work would be the comparison of the specific energy consumption in SWRO plants without energy recovery systems. The results of the *ROSA* and *Desal* software for hypothetical RO plant are presented in Table 5. In these hypothetical situations no energy recovery system is used and the plant design was kept the same as for the 280 m^3/day. The feed flow rate was kept constant at 40 m^3/h and a variable pressure was applied at 23°C and $c_f = 42{,}000$ mg/lt.

Table 5. Predictions about the specific energy consumption of the 280 m^3/day SWRO plant at 23° with no energy recovery system

Q_p (m^3/h) *ROSA* 6.0	Q_p (m^3/h) *Desal*	Recovery *ROSA* 6.0	Recovery *Desal*	ΔP_{ef} (bar)	ξ (kWh/m^3) *ROSA* 6.0	ξ (kWh/m^3) *Desal*	n_2
7.14	7.70	0.179	0.193	50.00	9.73	9.02	0.8
8.31	8.83	0.208	0.221	53.00	8.85	8.34	0.8
9.44	9.89	0.236	0.247	56.00	8.24	7.86	0.8
10.51	10.88	0.263	0.272	59.00	7.80	7.53	0.8
11.53	11.82	0.288	0.296	62.00	7.47	7.28	0.8
12.49	12.71	0.312	0.318	65.00	7.23	7.10	0.8
13.41	13.54	0.335	0.339	68.00	7.04	6.97	0.8
14.28	14.32	0.357	0.358	71.00	6.91	6.89	0.8
15.10	15.06	0.378	0.377	74.00	6.81	6.82	0.8
17.87	15.75	0.447	0.394	77.00	6.74	6.79	0.8
18.72	18.35	0.468	0.459	90.00	6.68	6.81	0.8
20.42	19.97	0.511	0.499	100.00	6.80	6.95	0.8
22.85	22.48	0.571	0.562	120.00	7.29	7.41	0.8

It is apparent from the results of Table 5 that *ROSA* and *Desal* give the same predictions about the specific energy consumption. In Table 5 the applied pressure has exceeded the maximum pressure that this type of membranes can take (69 bar). It is notable that the specific energy consumption has a minimum at a particular applied pressure and recovery ratio, something that will be investigated in the following paragraph.

OPTIMIZATION OF THE DESIGN AND OPERATION OF RO PLANTS

The *Desal* software which is proposed in this work is a very useful tool for predicting the optimum design and operation of the SWRO plant. If one considers the commercial plant examined in this work, with no energy recovery system and ignores the auxiliary devices, an optimum recovery ratio, R, can be found for the minimum specific energy consumption, ξ. In Fig. 5 predictions have been made about ξ as a function of the recovery ratio at every constant feed flow rate. It is interesting that a minimum specific energy consumption is achieved at $R = 0.43-0.46$. The applied pressure is around 80 bar, for this particular type of membranes and SWRO plant. However, the applied pressure and the feed flow rate are limited by the mechanical strength of the membrane and the active layer as well as the scale formation.

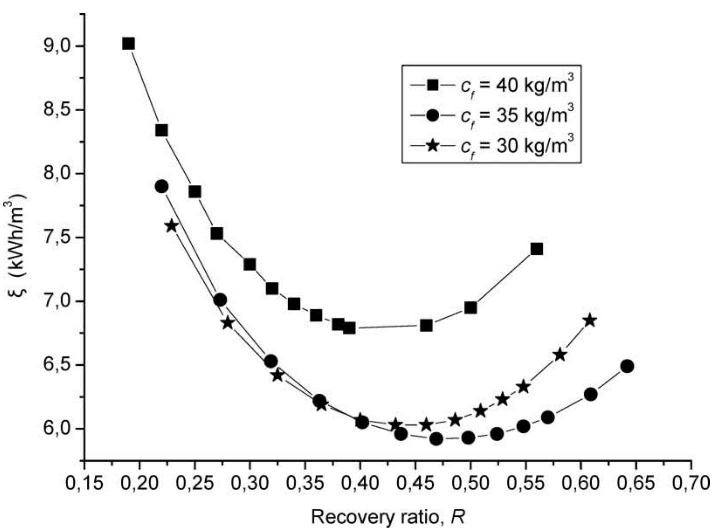

Figure 5. Specific energy consumption for different recoveries at constant feed flow rate at 23°C.

In Fig. 6 the specific energy consumption is given as a function of the recovery ratio, which is dictated by the feed flow rate at different but reasonable applied pressures. As it was expected the higher the recovery, R, the lower the specific energy, ξ. This means that at constant applied pressure as the feed flow rate decreases the specific energy, ξ, decreases as well. On the other hand the permeate concentration is another factor that put a limit to the recovery ratio regardless of the energy savings. In the data illustrated in Fig. 6 if the feed flow rate is set to $Q_f = 10\,m^3/h$ the permeate concentration is calculated to $c_p = 2547\,mg/lt$, which is an unacceptable value. As it was mentioned before, the scale formation is another factor that should be taken into account as it puts a limit to the recovery ratio. However, in real life the productivity of a plant in order to meet the demand may be more important than the specific energy consumption.

Another parameter which can be investigated in this work is the number of membrane modules in the pressure vessel. It is expected that as the number of membrane modules increases the recovery ratio increases as well and consequently the specific energy consumption will decrease. In Fig. 7 two different operating conditions were used. The one is the actual operating conditions of the $280\,m^3/day$ SWRO and the other is the operational limits for this type of membranes (SW30HR380). All the calculations concern SWRO plant with four pressure vessels with membranes. It can be seen that there is a great reduction in specific energy as the number of membrane modules increase. When 10 membrane modules are used the recovery ratio is about $R = 0{,}36$ and the specific energy consumption about $6\,kWh/m^3$. The number of the membrane modules is limited again by the productivity of the membranes.

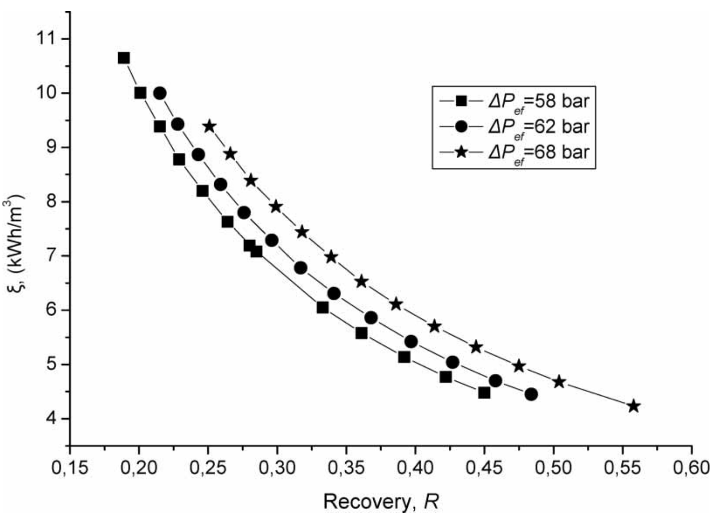

Figure 6. Specific energy consumption for different recoveries at constant feed pressure at 23°C.

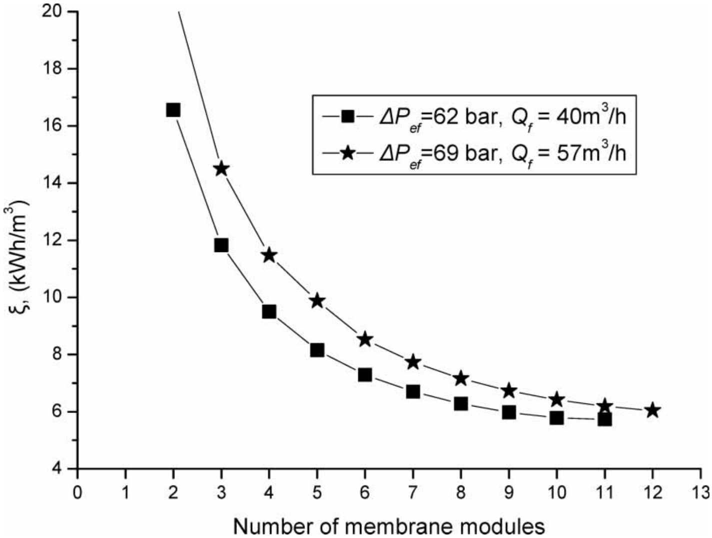

Figure 7. Specific energy consumption for different number of membrane modules at 23°C.

The last membranes because of the high recovery and concentration polarization effects produce less water than normally. However, the decrease in specific energy consumption is rather caused by the increased number of membranes in use and the higher recovery ratio. If the same number of membranes are used in different configuration then it seems that the configuration with many successive membrane modules is slightly more effective. As an example 24 membrane modules are set in two different configurations: six pressure vessels with four membranes each one, and three pressure vessels including eight membranes each. For seawater feed with concentration $c_f = 42{,}000\,\mathrm{mg/lt}$ at 62 bar, 23°C and $Q_f = 40\,\mathrm{m^3/h}$ the *Desal* software predicts that in the first configuration $Q_p = 11.57\,\mathrm{m^3/h}$ and $c_p = 240\,\mathrm{mg/lt}$, though in the second configuration $Q_p = 11.82\,\mathrm{m^3/h}$ and $c_p = 262\,\mathrm{mg/lt}$. The above results show that the configuration of the membrane modules is rather dictated by other factors such as the cost of the parts and the pressure vessels, the available space etc.

CONCLUSIONS

An explicit analytical mathematical model has been used to develop a simple software for the prediction of the SWRO plants performance. The mathematical model and the software were verified on experimental data taken from a $280\,\mathrm{m^3/day}$ plant and a very good agreement with them was found. The predictions of SWRO plants in this work are similar to the prediction of *ROSA* 6.0 software, developed by FilmTec for the membranes used in the experiments. After a thorough investigation of optimum operating condition it was concluded that the reduction of the specific energy consumption for the SW30HR380 membranes can be achieved by operating the plant at recovery around 0.45. Although there are new membranes with low energy consumption in the market, it is postulated that if SW30HR380 membrane modules had higher mechanical strength and capability to sustain 90 bar pressure then a lower specific energy consumption could be achieved. It has been shown that the membrane modules arrangement has a minor effect on the specific energy consumption.

SYMBOLS

c	concentration, kg m^{-1}
f	constant defined by Eqn. (A.2), kg m^{-4}
ΔP_{ef}	driving Pressure, Pa
ΔP	pressure difference given by $(P_f - 10^5)$, Pa
ΔP_{pump}	Applied pressure only by the high pressure pump, Pa
f	concentration gradient coefficient, kg m^{-4}
h	height, m
I	electrical current, A
J	average volumetric flux, m s^{-1}
J_2	average solute mass flux, kg m^{-2} s^{-1}
k	mass transfer coefficient, m s^{-1}
k_1	water permeability coefficient, m s^{-1} Pa^{-1}
k_2	solute permeability coefficient, m s^{-1}
k_f	friction parameter, m^{-2}
L	membrane length (axial), m
L_2	membrane length with glue, m
n_1	efficiency coefficient of HP pump
n_2	efficiency coefficient of auxiliary devices
P	electrical power, kW
P_f	applied pressure at the inlet of the pressure vessel, Pa
P^0	constant (10^5 Pa)
q	constant for a given membrane and temperature, defined by Eqn. (4), m
Q	flow rate, m^3/s
R	recovery ratio
Re	Reynolds number ($Re = hu\rho/\mu$)
Sc	Schmidt number ($Sc = \mu/\rho D$)
Sh	Sherwood number ($Sh = kh_b/D$)
t	number of membrane modules in the pressure vessel
T	temperature, K
U	voltage, V
u	velocity, m/s

w	membrane width (tangential), m
w_2	membrane width with glue, m
x	coordinate along the membrane length, m
y	coordinate along the membrane width, m

Greek Letters

μ	viscosity, kg m^{-1} s^{-1}
ξ	specific energy consumption, kWh/m^3
π	osmotic pressure, Pa
ρ	density, kg/m^3
ω	osmotic pressure coefficient, N m kg^{-1}

Subscript

b	brine
ef	effective
f	feed
m	membrane
p	permeate
w	wall

Appendix. Dimensions of the 8″ SW30HR380 modules

Permeate channel height (mm)	$h_p = 0.52$
Brine channel height (mm)	$h_b = 0.84$
Membrane height (mm)	$h_m = 0.14$
Total membrane length (cm)	$L_2 = 96.50$
Active membrane length (cm)	$L = 86.65$
Total membrane width (cm)	$w_2 = 134$
Active membrane width (cm)	$w = 117$
Active membrane area (m^2)	$A = 26{,}35$
Number of leaves in 8″ SW30HR380	$N = 13$

ACKNOWLEDGMENTS

The author expresses his gratitude to Mr. M. Pitsikalis for his support in the experimental part of this work.

REFERENCES

1. Wilf, M. (1997) Design consequences of recent improvements in membrane performance. *Desalination*, 113: 157–163.
2. Busch, M. and Mickols, W.E. (2004) Reducing energy consumption in seawater desalination. *Desalination*, 165: 299–312.

3. Al-Hawaj, O.M. (2003) The work exchanger for reverse osmosis plants. *Desalination*, 157: 23–27.
4. Thomson, M., Miranda, M.S., and Infield, D. (2002) A small scale seawater reverse osmosi system with excellent energy efficiency over a wide operating range. *EUROMED 2002*; Sharm El-Sheikh: Egypt, May 4–6.
5. Rautenbach, R. and Dahm, W. (1989) Design and optimization of spiral wound and hollow fibers RO modules. *Desalination*, 65: 299–275.
6. Avlonitis, S.A. et al. (1991) Spiral wound modules performance. An analytical solution: Part I. *Desalination*, 81: 191–208.
7. Ben Boudinar, M. et al. (1992) Numerical simulation and optimization of spiral wound modules. *Desalination*, 86: 273–290.
8. Avlonitis, S.A. et al. (1993) Spiral wound modules performance. An analytical solution: Part II. *Desalination*, 89: 227–246.
9. Avlonitis, S. et al. (1995) Optimal design of spiral wound modules: an analytical method. *Chemical Eng. Research and Design*, 73 (PartA): 575–581.
10. Evagelista, F. and Jonsson, G. (1988) Optimal design and performance of spiral wound modules. *Chemical Eng. Com.*, 72: 69–81.
11. Avlonitis, S. et al. (2003) energy consumption and membrane replacement cost for seawater RO desalination plants. *Desalination*, 157: 151–158.
12. Wilf, M. and Klinco, K. (2001) Optimization of seawater RO systems design. *Desalination*, 138: 299–306.
13. Mesa, A.A. et al. (1996) Design of the maximum energy efficiency desalination plant (PAME). *Desalination*, 108: 111–116.
14. Feth, K. (2003) Optimization of energy consumption in the 3300 m^3/d RO Kerkennah plant. *Desalination*, 157: 145–149.
15. Hafsi, M.M.M. and Boughriba, A. (2002) Five years experience in reverse osmosis plant optimization performances in Morocco. *Desalination*, 153: 227.
16. Manth, T., Gabor, M., and Oklejas, E., Jr. (2003) Minimizing RO energy consumption under variable conditions of operation. *Desalination*, 157: 9–21.
17. Villafafila, A. and Mujtaba, I.M. (2003) Fresh water by reverse osmosis based desalination: simulation and optimization. *Desalination*, 155: 1–13.
18. Geraldes, V. et al. (2005) Simulation and optimization of medium-sized seawater reverse osmosis processes with spiral-wound modules. *Ind. Eng. Chem. Res.*, 44: 1897–1905.
19. Uche, J. et al. (2003) Software for the analysis of water an energy systems. *Desalination*, 156: 367–378.
20. Baker, E.C., Moosemiller, M.D., and Mustakas, G.C.. Computer optimization of reverse osmosis processing of soy whey with cellulose acetate module. *Journal of Applied Polymer Science*, 24 (3): 749–762.